Journal of the Serbian Chemical Society
Electronic Version
JSCS-info@shd.org.rs • www.shd.org.rs/JSCS

ACCEPTED MANUSCRIPT

This is an early electronic version of an as-received manuscript that has been accepted for publication in the Journal of the Serbian Chemical Society but has not yet been subjected to the editing process and publishing procedure applied by the JSCS Editorial Office.

Please cite this article as S. K. Belošević, S. B. Novaković, M. V. Rodić, V. M. Leovac, Lj. S. Vojinović-Ješić, G. A. Bogdanović, and M. M. Radanović, *J. Serb. Chem. Soc.* (2024) https://doi.org/10.2298/JSC240417050B

This "raw" version of the manuscript is being provided to the authors and readers for their technical service. It must be stressed that the manuscript still has to be subjected to copyediting, typesetting, English grammar and syntax corrections, professional editing and authors' review of the galley proof before it is published in its final form. Please note that during these publishing processes, many errors may emerge which could affect the final content of the manuscript and all legal disclaimers applied according to the policies of the Journal.

Journal of the Serbian Chemical Society
JSCS-info@shd.org.rs • www.shd.org.rs/JSCS

J. Serb. Chem. Soc. **00(0)** 1-14 (2024)
JSCS–12896

Original scientific paper
Published DD MM, 2024

Introducing a novel crystal form of pyruvic acid thiosemicarbazone and its sodium salt

SVETLANA K. BELOŠEVIĆ[1#], SLAĐANA B. NOVAKOVIĆ[2]*, MARKO V. RODIĆ[3#], VUKADIN M. LEOVAC[3#], LJILJANA S. VOJINOVIĆ-JEŠIĆ[3#], GORAN A. BOGDANOVIĆ[2], AND MIRJANA M. RADANOVIĆ[3]**[#]

[1]*Faculty of Technical Sciences, University of Priština, Knjaza Miloša 7, 38220 Kosovska Mitrovica, Serbia,* [2]*"Vinča" Institute of Nuclear Sciences - National Institute of the Republic of Serbia, University of Belgrade, P. O. Box 522, 11001 Belgrade, Serbia,* [3]*University of Novi Sad, Faculty of Sciences, Trg Dositeja Obradovića 3, 21000, Novi Sad.*

(Received 17 April; revised 21 April; accepted 8 May 2024)

Abstract: The reaction of thiosemicarbazide and sodium pyruvate has been thoroughly studied and the novel crystal form of pyruvic acid thiosemicarbazone (H_2pt) and its sodium salt were obtained. Compounds were characterized by IR spectra, melting points, elemental analysis and conductometric measurements, as well as single-crystal X-ray analysis. A detailed comparative analysis of crystal structures of these compounds is given, as well as comparison with some of the earlier known complexes containing H_2pt. The two novel crystal structures exhibit notably different hydrogen bonding patterns, mutually and in comparison with previously reported crystal form of H_2pt. All crystal structures are stabilized by extensive network of N–H...O, O–H...O and N–H...S hydrogen bonds. The cyclic hydrogen bonding motif involving the thioureido moieties of the ligand is the only one which repeats in each structure.

Keywords: thiosemicarbazone; crystal structure; physicochemical properties; metal complexes; hydrogen bonding.

INTRODUCTION

Thiosemicarbazones are a versatile class of compounds with a very wide range of biological activities and numerous potential applications in pharmacology and medicine[1-5], as well as analytical chemistry[6-8] and industry.[9, 10] The majority of these remarkable features arise from the ability of thiosemicarbazones [$R_1R_2C{=}N^1N^2(H)C(S)N^3H_2$] to strongly coordinate the transition metal ions. The coordination usually occurs through the hydrazine N1 and thioamide S donors, while other coordination modes are also available due to several potential donor

* Corresponding authors. E-mail: snovak@vin.bg.ac.rs; ** mirjana.lalovic@dh.uns.ac.rs
https://doi.org/10.2298/JSC240417050B
[#]Serbian Chemical Society member

atoms in the thiosemicarbazone moiety.[11, 12] Another very important feature of thiosemicarbazones is their great structural variety achieved by the variation of residues attached to the NNCS system. Thus, the thiosemicarbazone ligands, which are generally obtained in the condensation reaction of thiosemicarbazide and different aldehydes and ketones, also incorporate additional coordination and/or interaction sites available at the carbonyl residues.[11-13] Equally important as the coordination and structural variety is the ability of thiosemicarbazones to form extensive hydrogen bonding with the closest environment. This is of primary importance for biologically active molecules where the non-covalent interactions lead the molecule recognition processes with the biological systems.[14-16]

As the properties of thiosemicarbazones are dependable on their carbonyl residues, a vast number of carbonyl compounds have been used in their synthesis, including the keto-acids. Among the ligands of the latter type, particular attention has been paid to the pyruvic acid thiosemicarbazone and its complex compounds due to their evident biological activity.[17-21] Pyruvic acid is the simplest of the alpha-keto acids, known as an important component in several metabolic processes within the living cell. Apart from incorporating biologically relevant fragment, the corresponding pyruvic acid thiosemicarbazone gains additional coordination sites in the form of two oxygen donors from the carboxylic group. Moreover, the pyruvic acid thiosemicarbazone, a relatively small size molecule, joins together three very interactive fragments, viz. hydrazine, thioamide, and carboxylate, all with exceptional hydrogen bonding ability. This feature certainly increases the ability for intermolecular interactions, as well as the possibility for polymorphic crystallization.

This paper presents a novel synthetic route for the pyruvic acid thiosemicarbazone ligand. The structural analysis of the obtained compound revealed that this is actually a new crystal form of the pyruvic acid thiosemicarbazone (H_2pt), dissimilar to the previously reported crystal structure[22] (CSD refcode[23]: YEBBUC). In addition, the study includes novel crystal structure of the sodium salt of pyruvic acid thiosemicarbazone, which is one of very rare crystal structures of the alkali and earth-alkali compounds with the thiosemicarbazone ligands in general. Considering the significance of different crystal forms and dissimilar intermolecular arrangements for properties such as biological activity and solubility, in the present study we aim to compare remarkable hydrogen bonding features in different crystal forms of H_2pt and its sodium salt.

EXPERIMENTAL

Materials and physical measurements

All starting materials and solvents were purchased from Sigma-Aldrich Chemical Company and were used without further purification. C, H, N, and S elemental analyses were performed by standard micro-methods in the Center for Instrumental Analysis, ICTN, in

Belgrade. Melting points were measured with a Nagema PHMT 05 hot-stage microscope. IR spectra were carried out in a range of 400-4000 cm^{-1} using Nicolet Nexus 670 FTIR (Thermo Scientific) spectrophotometer. The molar conductivity measurements of freshly prepared solutions (c = 1 mmol L^{-1}) were performed on a Jenway 4510 conductivity meter.

*Preparation of $H_2pt{\cdot}0.5H_2O$ (**1**)*

The initial solution of H_2pt was obtained in the reaction of a mildly heated aqueous solution (5 cm^3) of thiosemicarbazide hydrochloride (0.64 g, 5 mM) and an aqueous solution (5 cm^3) of sodium pyruvate (0.55 g, 5 mM). The mixture was mildly heated for about 3 minutes. The obtained white microcrystalline product was filtered off after 24h and washed with water. Yield: 55 %. Anal. Calc. for $C_4H_7N_3O_2S{\cdot}0.5H_2O$ ($H_2pt{\cdot}0.5H_2O$): C, 28.23; H, 4.71; N, 24.71; S, 18,82 %. Found: C, 28.52; H, 4.60; N, 24.58; S, 18.74 %. M. p. 216 °C. Selected IR bands (cm^{-1}): 3414_m, $\nu_a(H_2O)$; 3293_m, 3182_m, $\nu_s(NH_2/NH)$; 1727_s, 1699_{vs}, $\nu(CO)$ of COOH; 1614_{vs}, $\nu(CN)$; 802_m, $\nu(CS)$. A few single crystals suitable for X-ray analysis were obtained from the mixture of $CaCO_3$ (10 mg) and the obtained ligand (32 mg) in water (5 cm^3) heated at 60 °C for 15 min and then cooled to room temperature.

*Preparation of sodium pyruvate thiosemicarbazone $\{[Na(Hpt)(H_2O)_3]{\cdot}H_2O\}_n$ (**2**)*

The aqueous solution (5 cm^3) of equimolar amounts of sodium-pyruvate (0.55 g, 5mM) and thiosemicarbazide (0.46 g, 5 mM), was heated at 50 °C for about 1.5 h. After solvent evaporation at room temperature, obtained white single crystals were washed with EtOH-H_2O (1:1). Yield: 47 %. Anal. Calc. for $NaC_4H_8N_3O_3S{\cdot}3H_2O$: C, 20.70; H, 6.03; N, 18.10 %. Found: C, 20.55; H, 5.89; N, 18.01 %. M. p. 208 °C; λ_M [Scm^2mol^{-1}]: 87 (H_2O), 98 (MeOH). Selected IR bands (cm^{-1}): 3458_m $\nu(H_2O)$; 3366_m, 3315_m, 3141_m, $\nu(NH_2/NH)$; 1622_m, $\nu(CN)$; 1571_{vs}, $\nu_a(CO_2^-)$; 1381_{vs}, $\nu_s(CO_2^-)$; 789_m, $\nu(CS)$.

Crystal structure determination

The single-crystal X-ray diffraction data for **1** and **2** were collected using an Oxford Diffraction Gemini S diffractometer. The reflection integration and data reduction were performed with the CrysAlisPro.[24] The crystal structures were solved by direct methods and refined using full-matrix least-squares against F^2 with the SHELX programs.[25] The H atoms bonded to N and O atoms were located from difference Fourier maps and refined isotropically, or by applying DFIX restraints, with O–H and N–H distances restrained to 0.82(1) and 0.87(1) Å, respectively, and $U_{iso}(H) = 1.2U_{eq}(O, N)$. H atoms bonded to C atoms were introduced in idealized positions and treated with a riding model. Crystallographic and refinement details are given in Table S1 of the Supporting information file (SI). Mercury software[26] was used to analyze and graphically present the crystal structures. The CrystalExplorer[27] was employed to calculate intermolecular interaction energies at the B3LYP-D2/6-31G(d,p) level of theory using the crystal geometry. Crystallographic data associated with this publication are deposited with the Cambridge Crystallographic Data Centre under the CCDC Numbers 2347833 and 2347834. The data are available free of charge at https://www.ccdc.cam.ac.uk/structures.

RESULTS AND DISCUSSION

Syntheses and characterization

In Fig. 1. the synthesis of both known ligand forms and the sodium salt is presented. According to the previously described synthetic procedure[28, 29], the pyruvic acid thiosemicarbazone could be obtained from the aqueous solution of thiosemicarbazide hydrochloride and pyruvic acid. The same compound was

obtained here, by the reaction of aqueous solution of thiosemicarbazide hydrochloride and sodium-pyruvate. Interestingly, by heating the aqueous solution of the pyruvic acid thiosemicarbazone and $CaCO_3$, instead of the expected calcium salt, single crystals of a new crystal form of the initial ligand were obtained ($H_2pt \cdot 0.5H_2O$, **1**). On the other hand, the reaction of the warm aqueous solution of neutral thiosemicarbazide and sodium pyruvate resulted in the sodium salt of pyruvic acid thiosemicarbazone $\{[Na(Hpt)(H_2O)_3] \cdot H_2O\}_n$ (**2**). The molar conductivity of water and methanolic solutions of **2** corresponds to a 1:1 type of electrolyte.

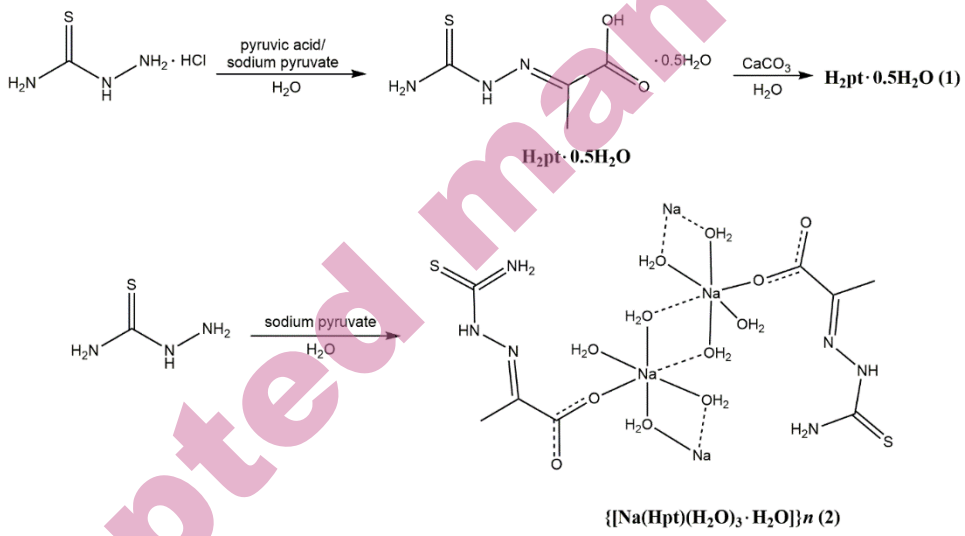

Fig. 1. Reaction scheme for obtaining H_2pt and its sodium salt

In most structures of metal complexes containing H_2pt, it is coordinated as a monoanionic or dianionic tridentate *ONS* ligand through the oxygen atom of the carboxyl group, the azomethine nitrogen atom, and the sulfur atom.[29, 30] However, in pentacoordinate $[Zn(H_2pt)(Hpt)Cl]$[30], aside from the tridentate coordination of Hpt^-, monodentate coordination of neutral H_2pt through the sulfur atom is found. In **2**, another mode of monodentate coordination of this ligand is found, i.e., coordination via the oxygen atom of the deprotonated carboxyl group (vide infra). Thus, in the IR spectra of **1** and **2** (Fig. S1 and S2, Supplementary Material), ν(C=N) and ν(C=S) bands are found at nearly the same wavenumbers. A significant difference can be observed in the positioning of carboxyl bands, found at 1727 and 1699 cm^{-1} in the spectrum of **1**, and 1571 cm^{-1}, $\nu_a(CO_2^-)$ and 1381 cm^{-1}, $\nu_s(CO_2^-)$ in the spectrum of **2**.

*Molecular structures of $H_2pt.0.5\ H_2O$ (**1**) and $\{[Na(Hpt)(H_2O)_3]\cdot H_2O\}_n$ (**2**)*

Crystal structures of **1** and **2** have been determined by single crystal X-ray analysis. The molecular structures of these compounds are presented in Fig. 2, while selected geometrical parameters are compared in Table I. Both compounds crystallize in the triclinic crystal system in space group $P\bar{1}$. The asymmetric unit of **1** contains two crystallographically independent molecules (denoted A and B) and a molecule of crystal water (Fig. 2a), dissimilar to its previously reported crystal form containing the three independent H_2pt molecules.[22] The compound **2** crystallizes as a coordination polymer with the Hpt^- anions neutralized by the solvated sodium counterions (Fig. 2b).

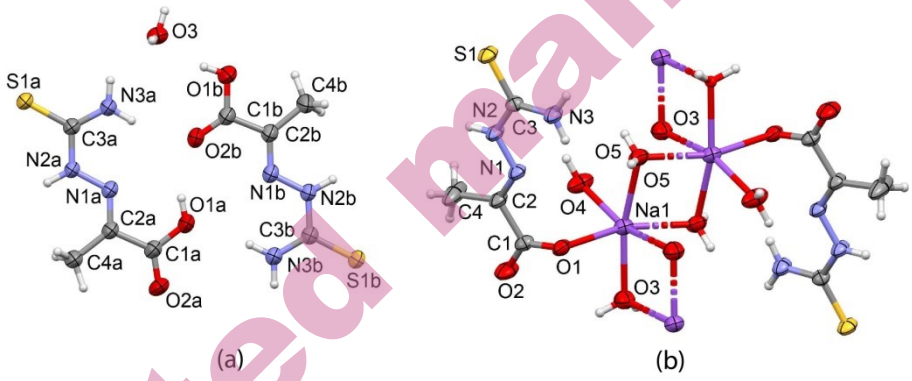

Fig. 2. Molecular structure of (a) **1** and (b) fragment of **2**.

At the molecular level, the neutral H_2pt ligand and its Hpt^- anion show little differences. The main structural feature of these molecules is their approximately planar form resulting from the intrinsic planarity of the pyruvate and thiosemicarbazide components. The dihedral angles between the best planes formed by the non-H atoms of two components are 4.21(8) and 5.02(8)° in independent molecules H_2pt_A and H_2pt_B, respectively and 1.6(1)° in the Hpt^- anion of the salt. Also, all molecules adopt the *E* configuration with respect to the C2–N1 and the C3–N2 bond. This arrangement places the N1 and S ligators on mutually opposite sides of the molecule, as typical for most uncoordinated thiosemicarbazone ligands (Fig. 2).

TABLE I. Selected geometric parameters (°, Å)

Bond (Å)	**1_A**	**1_B**	**2**
N1–N2	1.361(2)	1.361(2)	1.376(2)
N1–C2	1.283(2)	1.280(2)	1.272(2)
N2–C3	1.361(2)	1.320(2)	1.347(2)
N3–C3	1.312(2)	1.357(2)	1.312(2)
C3–S1	1.685(2)	1.686(2)	1.699(2)
C1–O1	1.329(2)	1.310(2)	1.258(2)
C1–O2	1.203(2)	1.212(2)	1.242(2)
Na1–O1	–	–	2.457(2)
<Na1–Ow>	–	–	2.314
Angle (°)	**1_A**	**1_B**	**2**
N1–N2–C3	118.6(2)	119.0(2)	118.3(2)
N2–C3–N3	117.3(2)	117.6(2)	117.9(2)
N2–C3–S1	119.3(2)	119.5(2)	119.2(2)
O1–C1–O2	119.0(2)	123.9(2)	125.4(2)

The bond lengths and angles of the three molecules, compared in Table I, confirm their close geometrical similarity. The bond distances are intermediate between those of single and double bonds, indicating the electron delocalization, as consistent with the molecular planarity. Among the three C–N bonds present in each molecule, the C2–N1, at the junction of two fragments, has the highest double bond character. A more significant bond length differences involve C–O bonds, which obviously differ in H_2pt molecules due to protonated O1 while having similar lengths in the anion. It is interesting to mention that intra-ligand bond lengths in **2** are in accordance with those found in the tridentate coordinated Hpt^- in [Zn(H_2pt)(Hpt)Cl].[30] The C–C bonds are single bonds allowing for free fragment rotation; indeed, the two independent molecules of H_2pt show different orientation of their carboxyl residues, with N1–C2–C1–O1 torsion angle of 179.0(1) and 4.8(2)° in molecules A and B, respectively.

In the crystal structure of **2**, the sodium ion is six-coordinated by one carboxylic oxygen atom from the thiosemicarbazone ligand and five oxygen atoms from the water molecules (Fig. 2b). Two of these water ligands have the role of the bridging ligands connecting the molecules into the one-dimensional chain, running along the *a* crystallographic axis. The Na–O bond distance involving the Hpt^- anion is 2.457(2) Å, while those to water molecules are 2.314 Å on average. The central part of the formed coordination polymer is composed of Na_2O_2 four-membered rings arranged at the dihedral angle of 77.7(1)°. The thiosemicarbazone ligand occupies the lateral sides of this chain and has a crucial role in the interconnection of chains by intermolecular interactions.

Comparison of crystal packing features

The crystal structures of **1** and **2** are both stabilized by the extensive network of N–H···O, O–H···O and N–H···S interactions. Deprotonation of H_2pt ligand and

the presence of additional water molecules in the sodium complex significantly change the hydrogen bonding pattern of pyruvate thiosemicarbazone relative to its neutral (acidic) form, despite the pronounced structural similarity of ligands at the molecular level. Nevertheless, even the two crystallographically independent molecules in the crystal structure of **1** (Fig. 2a) have notably different hydrogen bonding patterns, mainly related to the different orientations of their carboxylic groups. Thus, in molecule A, the carboxylic proton is oriented towards the hydrazine N1 atom to form an intramolecular O1a–H1a···N1a hydrogen bond, while in molecule B, the equivalent proton points out of the molecule to engage in short O1b-H1b···O3 interaction with the crystal water of the asymmetric unit (Fig. 2a).

There are two strong and directional N3–H···O hydrogen bonds (Table II) joining the pair of independent molecules within the asymmetric unit of **1**. Although the molecules A and B employ the equivalent thioamide N3–H donors, the dissimilar carboxylic oxygen atoms *i.e.* O1 and O2, serve as their acceptors (Fig. 3a). Viewed in terms of these N3–H···O interactions, the cyclic hydrogen bonding motif that links two independent molecules within the asymmetric unit of **1** can be described in Etter's graph-set notation[31] as $R^2_2(16)$, Fig 3a. In addition to the pair of N3–H···O interactions, the O1a–H donor, already engaged in the intramolecular O1a–H···N1a, also engages in O1a–H···O2b interaction, reinforcing the binding between the independent molecules. This is the only interaction in the crystal structure of **1** which directly links the two carboxyl groups. In combination with the above N3–H···O hydrogen bonds, the O1a–H···O2b gives rise to two smaller ring patterns, $R^1_2(10)$ and $R^2_2(10)$, Fig. 3a. From an energy standpoint (Table III), this molecular pair exhibits the highest binding affinity ($E = -64$ kJ mol^{-1}), with electrostatic interactions notably prevailing. This dominance is anticipated due to the mediation of two robust hydrogen bonds.

The remaining N3–H donor of molecule A interacts with the crystal water ($E = -27$ kJ mol^{-1}), while the equivalent N3–H donor of molecule B serves to connect the molecular pairs from the neighbouring asymmetric units through N3b–H3c···O2a interaction ($E = -30$ kJ mol^{-1}). Employing this latter interaction, the pairs of AB molecules arrange into tetramers, generating the cyclic hydrogen bonding motif $R^4_4(12)$, Fig. 3a.

TABLE II. Hydrogen bonding geometry (°, Å)

1	H···A	D···A	D-H···A	Symmetry codes
N3a–H3a···O2b	2.13(2)	2.98(2)	172(2)	x, y, z
N3b–H3d···O1a	2.13(2)	2.98(2)	172(2)	x, y, z
O1b–H···O3w	1.85(2)	2.65(2)	166(2)	x, y, z
O1a–H···O2b	2.02(2)	2.79(2)	155(2)	x, y, z
N3b–H3c···O2a	2.11(2)	3.00(2)	177(2)	−x+2, −y, −z+1
N2b–H···S1a	2.67(2)	3.54(2)	174(2)	x, y, z+1
N2a–H···S1b	2.62(2)	3.50(2)	174(2)	x, y, z−1
O3–H3···S1a	2.36(2)	3.176(2)	176(2)	−x+1, −y+2, −z
O3–H4···S1b	2.45(2)	3.246(2)	166(2)	−x+1, −y+1, −z+1
2	H···A	D···A	D-H···A	
O5–H6···O1	1.90(2)	2.736(2)	174(2)	x+1, y, z
O4–H4a···O2	1.87(2)	2.731(2)	171(2)	x+1, y, z
O4–H4b···O2	2.23(2)	2.933(2)	148(2)	−x+1, −y, -z+1
N3–H3a···O6	2.24(2)	3.070(2)	166(2)	x, y, z
O6–H6···N2	2.65(2)	3.182(2)	127(2)	x, y, z
N2–H2···S1	2.76(2)	3.584 (2)	173(2)	−x+2, −y, −z
N3–H3b···S1	2.59(2)	3.445 (2)	167(2)	−x+2, −y+1, −z

By contrast to present crystal structure **1**, the previously reported crystal form of H_2pt (CSD refcode YEBBUC, in further text H_2pt^Y) contains three symmetry independent molecules in the asymmetric unit, together with one molecule of crystal water. Though generally of the same types, the intermolecular interactions that stabilize the crystal structure of H_2pt^Y lead to notably different molecular arrangements in comparison to **1** (Fig. 3b). First of all, all three molecules of H_2pt^Y have an equivalent orientation of the carboxylic moiety with H donor engaged in intramolecular O1–H···N1 hydrogen bond. There are two hydrogen bonds mutually connecting the independent molecules A^Y and B^Y, the O1–H···O2 and N3–H···O2, both utilizing the O2 acceptor. The ring pattern $R^1_2(10)$ formed in this way is the only one based on N–H···O and O–H···O interactions that is common for **1** and H_2pt^Y (Fig. 3a,b). Contrary to **1**, the O1 of H_2pt^Y does not serve as an acceptor but only as an H-donor. Thus, two equivalent O1a–H···O2b and O1b–H···O2a interactions associate the pairs of independent molecules A^Y and B^Y into a tetramer, generating the ring motif $R^4_4(16)$ composed only of carboxylic residues (Fig. 3b). As regards the independent molecule C^Y, the both of its donor sites N1–H and O1–H are captured by the molecule of crystal water. The molecule C^Y links to the A^YB^Y -tetramer via the N3b–H···O2c interaction, where it provides the acceptor, Fig. 3b.

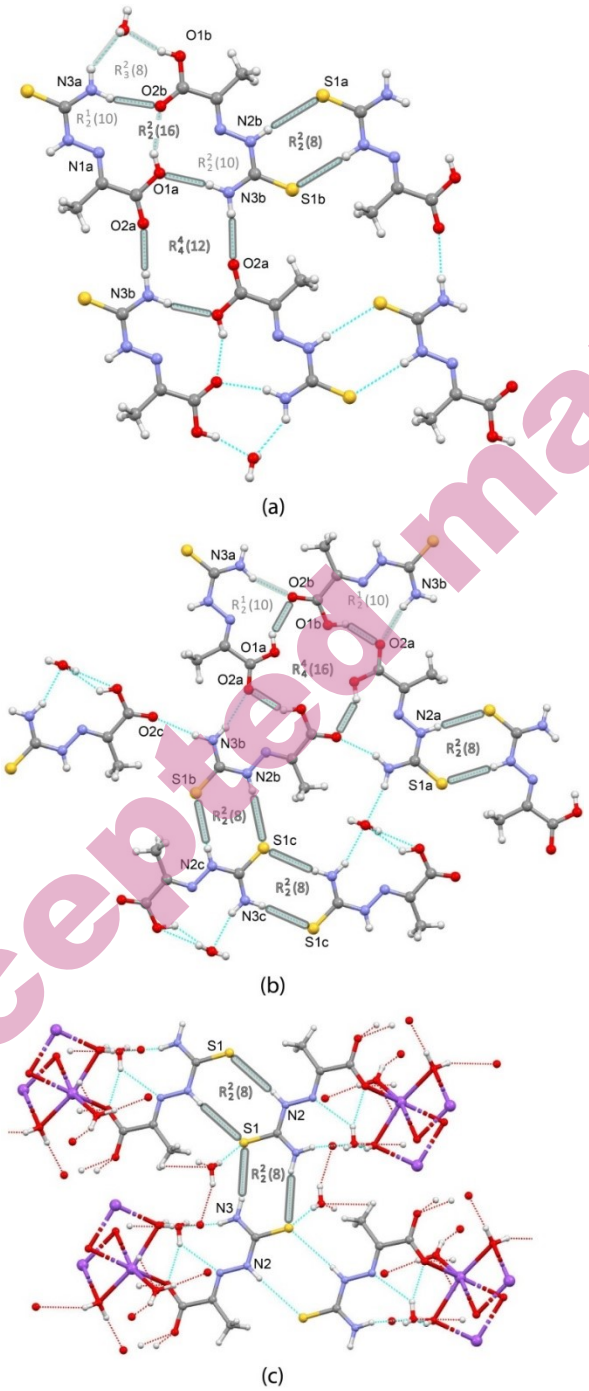

Fig. 3. Hydrogen bonding patterns in (a) $H_2pt\cdot0.5$ (**1**), (b) $H_2pt^{Y}\cdot0.33H_2O$[22] and (c) $\{[Na(Hpt)(H_2O)_3]\cdot H_2O\}_n$ (**2**). The ring patterns composed of one type of hydrogen bond are marked with ticker lines.

All molecules belonging to crystal structures of **1** and H_2pt^Y utilize their thiourea moieties to mutually connect by cyclic N–H···S hydrogen bonds (Fig. 3). In the structure of **1**, energy of this molecular dimer is estimated to −43 kJ mol^{-1}, mediated by N2a–H2a…S1b hydrogen bond. The $R^2_2(8)$ ring motif formed by these interactions frequently appears in thiosemicarbazide-based crystal structures in general.[32] In **1** and H_2pt^Y, all molecules form the $R^2_2(8)$ motif by the pairs of N2–H···S interactions. The exception is molecule C^Y, which, besides this one, forms the additional $R^2_2(8)$ motif utilizing centrosymmetric N3–H···S interaction (Fig. 3b).

Apart from the described interactions facilitated by hydrogen bonds, which orient molecules of **1** to form a sheet approximately parallel to the (940) crystallographic plane, three energetically comparable interactions emerge that are not reliant on specific atom-to-atom contacts. These interactions occur between stacked molecules. Unlike the electrostatically dominated interactions mediated by hydrogen bonds, these stacking interactions exhibit a comparable contribution from the dispersion component (Table III). These interactions, characterized by cohesion energies ranging from −20 to −30 kJ mol^{-1}, are the driving force behind the stacking of hydrogen-bonded layers, as opposed to the O–H···S hydrogen bond with an estimated energy of −12 kJ mol^{-1}.

TABLE III. Summary of relevant intermolecular interaction energies molecular pairs for **1**

X···*Y*	Symmetry operation on *Y*	Interactions involved	*R* / Å	*E* / kJ mol−1				
				E_{ele}	E_{pol}	E_{dis}	E_{rep}	E_{tot}
A···B	*x, y, z*	N3a–H3a···O2b O1a···H3d–N3b O1a–H1a···O2b	5.82	−80.59	−20.57	−20.44	87.91	−63.92
A···B	*x, y, z−1*	N2a–H2a···S1b	6.51	−56.96	−9.80	−19.57	66.65	−43.35
B···H2O	*x, y, z*	O1b–H1b···O3	6.17	−62.64	−15.68	−5.59	64.64	−42.77
B···B	*−x+1, −y+1, −z+1*	stacking	4.42	−14.21	−2.35	−27.30	10.85	−33.84
B···A	*−x+2, −y, −z+1*	N3b–H3c···O2a	8.89	−35.70	−6.52	−8.85	32.39	−30.27
A…A	*−x+1, −y+1, −z*	stacking	5.20	−18.14	−5.46	−23.67	24.59	−28.64
A···H_2O	*x, y, z*	N3a–H2b···O3	5.21	−28.07	−5.26	−4.70	16.82	−27.27
A···B	*−x+2 −y+1, −z+1*	offset stacking	5.88	−14.47	−3.60	−13.63	7.90	−24.96

X, *Y* are two molecules in interaction; *R* is the distance between molecular centroids. $E_{tot} = k_{ele}E_{ele} + k_{pol}E_{pol} + k_{dis}E_{dis} + k_{rep}E_{rep}$, where $k_{ele} = 1.057$, $k_{pol} = 0.740$, $k_{dis} = 0.871$, and $k_{rep} = 0.618$ for the B3LYP/6-31G(d,p) energy model used. Only Intermolecular energies with $-E > 25$ kJ mol^{-1} are listed.

In the crystal structure of **2**, there are five water molecules in the coordination environment of the sodium ion and the molecule of crystal water (Fig. 2b). Therefore, the O–H···O hydrogen bonds interconnecting the water molecules within the coordination polymer seem to dominate this crystal structure (Table II). In the dense network of O–H···O interactions, the Hpt^- anion participates with both oxygen acceptors of the deprotonated carboxyl group (Fig 3c). The coordination of Hpt^- to solvated sodium cation reduces the number of direct interactions between the thiosemicarbazone units. Nevertheless, the thiourea moieties of Hpt^- again self-associate using the N–H···S interactions to form a well-known $R^2_2(8)$ ring motif (Fig 3c). Similarly to C^Y from H_2pt^Y, the Hpt^- anion can form two of these motifs, one by N2–H···S and the other by N3–H···S interaction. In the crystal structure of **2**, these hydrogen bonds have the role of connecting the neighboring polymeric chains.

Apart from the extensive hydrogen bonding network and persistent $R^2_2(8)$ motif formed by thiourea moieties, the common feature of three crystal structures is their layered three-dimensional crystal packing. Fig. 4 displays 3D structure for compounds **1** and **2**. The layered structure is not surprising considering the planar form of the pyruvate thiosemicarbazone unit and the coplanarity of its hydrogen bonding sites, with the exception of methyl H atoms. The distance between two successive layers of ligands is 3.46, 3.34, and 3.64 Å in **1**, $H_2pt^Y{\cdot}0.33H_2O$, and **2**. The layers are interconnected by the hydrogen bonds involving water molecules (Fig. 4).

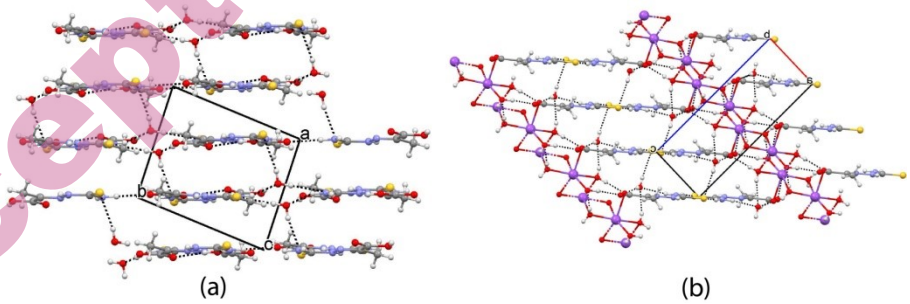

Fig. 4. Packing diagram of (a) **1** and (b) **2**.

CONCLUSION

By exploring novel synthetic routes for thiosemicarbazones with keto acids, and their complex salts with alkali and earth-alkali metals, we were able to isolate novel crystal form of pyruvic acid thiosemicarbazone, dissimilar to the previously reported crystal structure of this ligand. The sodium pyruvate thiosemicarbazone was also obtained in the form of a single crystal. Here presented crystal structure

of the sodium complex is one of very rare crystal structures of alkali and earth-alkali complexes of thiosemicarbazone ligands in general.

The thiosemicarbazone molecules display rather consistent planar form, due to overall electron delocalization. The allowed rotation of carboxylic fragment and its deportonation particularly affect the hydrogen bonding pattern. A detailed comparison has been made regarding the remarkable diversity of hydrogen bonding in novel and previously reported crystal form of pyruvic acid thiosemicarbazone. The comparison to sodium salt is also performed. Among the number of structural patterns formed by N–H...O, O–H...O and N–H...S interactions the cyclic hydrogen bonding motif involving thioureido moieties is the only one common for three crystal structures.

SUPPLEMENTARY MATERIAL

Additional data are available electronically at the pages of journal website: https://www.shd-pub.org.rs/index.php/JSCS/article/view/12896, or from the corresponding author on request.

Acknowledgements: This work was supported by the Ministry of Science, Technological Development and Innovation of the Republic of Serbia (Grant Nos. 451-03-66/2024-03/200017; 451-03-66/2024-03/200125 and 451-03-65/2024-03/200125).

И З В О Д

НОВА КРИСТАЛНА ФОРМА ТИОСЕМИКАРБАЗОНА ПИРОГРОЖЂАНЕ КИСЕЛИНЕ И ЊЕГОВЕ СОЛИ НАТРИЈУМА

СВЕТЛАНА К. БЕЛОШЕВИЋ[1#], СЛАЂАНА Б. НОВАКОВИЋ[2*], МАРКО В. РОДИЋ[3#], ВУКАДИН М. ЛЕОВАЦ[3#], ЉИЉАНА С. ВОЈИНОВИЋ-ЈЕШИЋ[3#], ГОРАН А. БОГДАНОВИЋ[2], И МИРЈАНА М. РАДАНОВИЋ[3*#]

[1]Факултет техничких наука, Универзитет у Приштини, Књаза Милоша 7, 38220 Косовска Митровица; [2]Институт за нуклеарненауке „Винча" – Институт од националног значаја за Републику Србију, Универзитет у Београду, Лабораторија за теоријску физику и физикукондензоване материје, 11001 Београд; [3]Универзитет у Новом Саду, Природно–математички факултет, Трг Д. Обрадовића 3, 21000 НовиСад

Детаљно је анализирана реакција тиосемикарбазида и натријум-пирувата, као и нова кристална форма добијеног тиосемикарбазона пирогрожђане киселине (H_2pt) и његове соли натријума. Једињења су окарактерисана IR спектроскопијом, елементалном анализом, кондуктометријом и рендгенском структурном анализом. Дата је упоредна анализа кристалних структура нових једињења, и њихова својста су упоређена са претходно описаним комплексима који садрже H_2pt. Две нове кристалне структуре показују значајне разлике у обрасцима водоничних веза, како међусобно тако и у поређењу са претходно описаном кристалном формом H_2pt. Све кристалне структуре су стабилизоване разгранатом мрежом N–H···O, O–H···O и N–H···S водоничних веза. Циклични мотив водоничних веза који укључује тиоамидне фрагменте лиганда је једини структурни мотив који се понавља у три упоређене кристалне структуре.

(Примљено 17. априла; ревидирано 21. априла; прихваћено 8. маја 2024.)

REFERENCES

1. A. Gómez Quiroga, C. Navarro Ranninger, *Coord. Chem. Rev*. **248** (2004) 119 (https://doi.org/10.1016/j.cct.2003.11.004)
2. G. L. Parrilha, R. G. dos Santos, H. Beraldo, *Coord. Chem. Rev*. **458** (2022) 214418 (https://doi.org/10.1016/j.ccr.2022.214418)
3. H. Beraldo, D. Gambino, *Mini-Rev. Med. Chem*. **4** (2004) 31 (https://doi.org/10.2174/1389557043487484)
4. D.S. Kalinowski D. R.Richardson, *Pharmacol. Rev*. **57** (2005) 547 (https://doi.org/10.1124/pr.57.4.2)
5. A. Mushtaq, P. Wu, M. M. Naseer, *Pharmacol. Ther*. **254** (2024) 108579 (https://doi.org/10.1016/j.pharmthera.2023.108579)
6. O. Özbek, C. Berkel, *Polyhedron* **238** (2023) 116426 (https://doi.org/10.1016/j.poly.2023.116426)
7. L. Feng, W. Shi, J. Ma, Y. Chen, F. Kui, Y. Hui, Z. Xie, *Sens. Actuators B: Chemical* **237** (2016) 563 (https://doi.org/10.1016/j.snb.2016.06.129)
8. R. Basri, N. Ahmed, M. Khalid, M. Usman Khan, M. Abdullah, A. Syed, A. M. Elgorban, S. S.Al-Rejaie, A. A. C. Braga, Z. Shafq, *Sci. Rep.* **12** (2022) 4927 (https://doi.org/10.1038/s41598-022-08860-3)
9. E. Khamis, M. A. Ameer, N. M. AlAndis, G. Al-Senani, *Corrosion* **56** (2000) 127 (https://doi.org/10.5006/1.3280528)
10. Q. A. Jawad, D. S. Zinad, R. D. Salim,A. A Al-Amiery,T. S. Gaaz,M. S. Takriff, A. A. H. Kadhum, *Coatings* **9** (2019) 729 (https://doi.org/10.3390/coatings9110729)
11. T. S. Lobana, R. Sharma, G. Bawa, S. Khanna, *Coord. Chem. Rev*. **253** (2009) 977 (https://doi.org/10.1016/j.ccr.2008.07.004)
12. J.S. Casas, M.S. Garcia-Tasende, J. Sordo, *Coord. Chem. Rev.* **209** (2000) 197 (https://doi.org/10.1016/S0010-8545(00)00363-5)
13. D. X. West, S. B. Padhye, P. B. Sonawane, *Struct. Bond*. **76** (1991) 1 (https://doi.org/10.1007/3-540-53499-7_1)
14. J. Haribabu, K. Jeyalakshmi, Y. Arun, N. S. P. Bhuvanesh, P. T. Perumal, R. Karvembu, *RSC Adv.* **5** (2015) 46031 (https://doi.org/10.1039/C5RA04498G)
15. L. R. P. de Siqueira, P. A. T. de Moraes Gomes, L. P. de Lima Ferreira, M. J. B. de Melo Rêgo, A. C. L. Leite, *Eur. J. Med. Chem.* **170** (2019) 237 (https://doi.org/10.1016/j.ejmech.2019.03.024)
16. H. Dong, J. Liu, X. Liu, Y. Yu, S. Cao, *Bioorg. Chem.* **75** (2017) 106 (https://doi.org/10.1016/j.bioorg.2017.07.002)
17. J. Wiecek, V. Dokorou, Z. Ciunik, D. Kovala-Demertzi, *Polyhedron* **28** (2009) 3298 (https://doi.org/10.1016/j.poly.2009.05.012)
18. M. B. Ferrari, F. Bisceglie, G. Pelosi, P. Tarasconi, R. Albertini, S. Pinelli, *J. Inorg. Bioch*. **87** (2001) 137–147 (https://doi.org/10.1016/S0162-0134(01)00321-X)
19. I. Graur,T. Bespalova, V. Graur, V. Tsapkov, O. Garbuz, E. Melnic, P. Bourosh, A. Gulea, *J. Chem. Res*. **47** (2023) 6 (https://doi.org/10.1177/17475198231216422)
20. T.A. Yousef, G.A. El-Reash, O.A. El-Gammal, R. A. Bedier. *J Mol Struct.* **1035** (2013) 307 (https://doi.org/10.1016/j.molstruc.2012.10.058)
21. N. I. Dodoff, D. Kovala-Demertzi, M. Kubiak, J. Kuduk-Jaworska, A. Kochel, G. A. Gorneva, *Z. Naturforsch. B* **61** (2006) 1110 (https://doi.org/10.1515/znb-2006-0909)
22. B. Ya.Antosyak, V. N. Biyushkin, L. F. Chapurina, T. I. Malinovsky, *Dokl. Akad. Nauk SSSR* **327** (1992) 219

23. C. R. Groom, I. J. Bruno, M. P. Lightfoot, S. C. Ward, *Acta Cryst*. **B72** (2016) 171. (https://dx.doi.org/10.1107/S2052520616003954)
24. CrysAlisPro 2021 Rigaku Oxford Diffraction Version 1.171.41.109a.
25. G. M. Sheldrick, *Acta Cryst.* **C71** (2015) 3 (https://doi.org/10.1107/S2053229614024218)
26. C. F. Macrae, I. Sovago, S. J. Cottrell, P. T. Galek, P. McCabe, E. Pidcock, P. A. Wood, *J. Appl. Cryst.* **53** (2020) 226 (https://doi.org/10.1107/S1600576719014092)
27. P. R. Spackman, M. J. Turner, J. J. McKinnon, S. K. Wolff, D. J. Grimwood, D. Jayatilaka, M. A. Spackman, *J. Appl. Cryst.* **54** (2021) 1006 (https://doi.org/10.1107/S1600576721002910)
28. G. L. Sawhney, J. S. Baijal, S. Chandra, K. B. Pandeya, *Acta Chim. Acad. Sci. Hung.* **108** (1981) 325
29. M. D. Timken, S. R. Wilson, D. N. Hendrickson, *Inorg. Chem*. **24** (1985) 3450 (https://dx.doi.org/10.1021/ic00215a030)
30. M. Belicchi Ferrari, Giovanna Gasparri Fava, G. Pelosi, P. Tarasconi, *Polyhedron* **19** (2000) 1895 (https://doi.org/10.1016/S0277-5387(00)00454-X)
31. M C Etter, J C MacDonald, J Bernstein, *Acta Cryst*. **B46** (1990) 256 (https://doi.org/10.1107/S0108768189012929)
32. S. B. Novaković, B. Fraisse, G. A. Bogdanović, A. Spasojevic-de Biré, *Cryst. Growth Des*. **17** (2007) 2993 (https://doi.org/10.1021/cg060497).